Non-perturbative treatment of particle dynamics in a semiclassical photon field

1987 J. Phys. B: At. Mol. Phys. 20 4441

(http://iopscience.iop.org/0022-3700/20/17/022)

J. Phys. B: At. Mol. Phys. **20** (1987) 4441-4452. Printed in the UK

Non-perturbative treatment of particle dynamics in a semiclassical photon field

Charles Cerjan† and Ronnie Kosloff‡

† Lawrence Livermore National Laboratory, University of California, Livermore, CA 94550, USA

‡ Fritz Haber Institute and Department of Chemistry, The Hebrew University, Jerusalem, Israel

Received 8 December 1986, in final form 27 March 1987

Abstract. A general calculational method is proposed to investigate the response of an electron residing in a one-dimensional potential well to an intense laser field. The numerical technique is based upon a psuedospectral solution of the time-dependent Schrödinger equation and is capable of incorporating the spatial and temporal aspects of the electromagnetic field. The intensity and frequency dependence of the ionisation rate along with the ejected-photoelectron spectrum are calculated for a one-dimensional cut-off harmonic-oscillator potential well.

1. Introduction

Stimulated by the ongoing experimental investigation of isolated atomic systems in intense laser fields (Kruit *et al* 1983, Luk *et al* 1985, Lompre *et al* 1985), many theoretical models have been proposed which examine different aspects of the particle-field interaction (Lambropolous 1985, Lambropolous and Smith 1985, L'Huillier *et al* 1986). Earlier work on time-dependent solutions to the Schrödinger equation for a particle in a semiclassical photon field has been constrained by the choice of numerical technique. One general approach, for example, which uses an integral equation formalism (Geltman 1977, Shakeshaft 1983), is limited by simplifying choices for the interaction potential and the necessity of assuming that the photon field is a perfect step function in time, i.e. no temporal (non-periodic) shape of a pulse can be readily considered within this formalism. This latter limitation is shared by time-independent Floquet analyses (Chu 1978, Muller and Tip 1984), which necessarily assume periodicity in the Hamiltonian function. In general, the difficulties experienced by all of these techniques are due to the difficulty of calculating the spatial matrix elements of a general potential, the choice of an initial state for the solution when the non-periodic temporal characteristics are important, the inapplicability of Floquet analysis and the convergence of a series expansion in terms of some small parameter.

In the following work, a general method is advanced which avoids all of these shortcomings. Additionally, this method is capable of incorporating many of the

0022-3700/87/174441+12$02.50

experimentally relevant, but theoretically intractable, quantities such as the temporal and spatial variation of the laser field. Likewise, it is not necessary to consider special limiting cases of high or low intensities, or large or small frequencies, in the analysis.

The approach taken in this work is to solve the time-dependent Schrödinger equation for the motion of a particle in a one-dimensional well in the presence of a time varying vector potential which describes the semiclassical electromagnetic field. This methodology permits the facile calculation of ionisation rates, time-averaged photoelectron peaks and various projections onto the stationary bound states of the system. In the following section the essential background for the solution of the one-dimensional Schrödinger equation will be described, details of the specific model and its solution will be given in § 3, results of the calculations will be presented in § 4 and the paper will conclude with a brief discussion of the limitations and possible extensions of this work.

2. Mathematical background

The essential idea behind the current approach is to solve the time-dependent Schrödinger equation directly without resorting to the usual basis state or Floquet expansion (Chu 1985). This technique is essentially complementary to these more standard methods since the continuum contribution is readily handled; however, the asymptotic analysis of the resulting time evolving wavefunction is more difficult.

The one-dimensional Hamiltonian chosen for this work is the usual non-relativistic description of a particle of mass m and charge $+e$ in a static well of potential $V(x)$, subjected to the time- and space-dependent electromagnetic vector potential field $A(x, t)$. With these assumptions, the Schrödinger equation is given by

$$i\hbar(\partial\varphi/\partial t)(x, t) = (\hbar^2/2m)(p - e/cA(x, t))^2\varphi(x, t) + V(x)\varphi(x, t). \tag{1}$$

The pA gauge and atomic units were selected for all the calculations performed.

The inherent difficulty of solving this partial differential equation is approached by the application of a psuedospectral, or fast Fourier transform (FFT), method for the spatial derivatives while retaining a simple explicit differencing scheme, or exponentiation (split-operator technique), for the time propagation. This method has been usefully employed in several other physical applications ranging from stationary-state evaluation to desorption and scattering from crystalline surfaces (Feit *et al* 1982, Tal-Ezer and Kosloff 1984, Kosloff and Cerjan 1984). This technique appears to be well suited for the examination of explicitly time-dependent Hamiltonian functions with few restrictions on the nature of those interactions.

Briefly, the method proceeds as follows. First, the Fourier transform of a wavefunction defined over a spatial grid at a specified time is taken; then this transform is multiplied by a power of ik; finally, the inverse Fourier transform of this product is evaluated. This process is summarised in the identity

$$\frac{\partial^{(n)}}{\partial x^{(n)}}\varphi(x, t) = \frac{\pi}{2}\int e^{-ikx}\int (ik)^n e^{iky}\varphi(y, t)\,dy\,dk \tag{2}$$

which is valid if the function $\varphi(x, t)$ vanishes on the grid boundary. In this way, a global representation of the spatial derivative is obtained on the grid. The remainder of the calculation is straightforward since the potential operator is strictly multiplicative

in this representation. The time evolution is provided by a simple two-point differencing scheme.

Expanding the full Hamiltonian function of equation (1) within the coordinate representation yields the equation

$$\frac{\hbar}{\mathrm{i}}\frac{\partial\varphi}{\partial t}=-\frac{\hbar^2}{2m}\frac{\partial^2\varphi}{\partial x^2}+\frac{\mathrm{i}e\hbar^2}{2mc}\varphi\left(\frac{\partial A}{\partial x}\right)+\frac{\mathrm{i}e\hbar^2}{mc}A\left(\frac{\partial\varphi}{\partial x}\right)+\frac{e^2\hbar^2}{2mc^2}A^2\varphi+V(x)\varphi. \tag{3}$$

In general, the vector potential $A(x, t)$ contains the spatial and temporal characteristics of the laser field and the inclusion of these features presents no difficulty for the psuedospectral technique. The spatial dependence of the vector field will be discussed in more detail later, but for the purposes of the present discussion, this is an unnecessarily general form since the photon frequencies considered here satisfy the usual conditions for the validity of the dipole approximation, $A(x, t)=A_0(t)\cos(\omega_p t)$, where ω_p is the photon frequency. The temporal shape of the pulse is incorporated by specifying a suitable functional form for $A_0(t)$.

The static potential $V(x)$ is similarly allowed to be quite general provided that it decays sufficiently fast at the boundary of the region. For the applications given below, this potential was chosen to be a cut-off harmonic oscillator

$$V(x)=\begin{cases}\frac{1}{2}m\omega_e^2x^2 & |x|\leqslant x_c\\ V_0 & |x|>x_c\end{cases} \tag{4}$$

where $\pm x_c$ is $(2V_0/m)^{1/2}/\omega_e$ to ensure continuity at $x=\pm x_c$. This model form has the advantage of having its stationary states close to the infinite harmonic well eigenstates and yet it permits photoionisation. There is no fundamental reason, though, for this preference since other forms, such as a finite square well or Eckart potential, produce qualitatively similar effects for similar parameter choices.

To summarise, this technique is applied in the following steps. Specific forms are chosen for $A(x, t)$ and $V(x)$ in equation (3) and these functions are evaluated on a suitable grid. A zero-time wavefunction—the initial state—is constructed on the grid. The spatial derivatives in equation (3) are evaluated by the procedure indicated in equation (2) at a specific time. Propagation in time is given by a two-point differencing formula controlled by a stable choice of time step so that the $(n+1)$th time step is given simply in terms of the nth step. The time propagation is repeated for the duration of the physical interaction. The steps followed here are discussed in more detail in a previous work (Kosloff and Kosloff 1983).

3. Computational details

The particular choices of the various terms in § 2 determine the model problem. For the first set of applications, the dipole approximation is employed with a hyperbolic-tangent initialisation function for the laser pulse. That is,

$$\begin{aligned}A(x, t)&\simeq A(t)\cos(\omega_p t)\\ &=A_0\tanh(\omega_p t/a)\cos(\omega_p t)\end{aligned} \tag{5}$$

where a is adjusted to produce a field of maximum intensity A_0 after a specified

number of field cycles. Typically, $a = 20\pi$. In principle, the laser field should also be terminated slowly but the timescales in these model calculations are so short that no physically realisable pulse would be decreasing in this time interval.

The static-potential parameters were selected to simulate two bound states in the Xe atom. That is, the cut-off harmonic well supports two eigenstates separated by 8.3 eV ($\omega_e = 0.3056$ Hartree) with a total well depth of 16.3 eV ($V_0 = 0.59857$ Hartree). The particle is chosen to be an electron ($m = 1$) initially in the ground state. The energies and zero-field stationary-state wavefunctions are readily calculated by propagating an initial guess for the wavefunction in imaginary time. This technique produces wavefunctions which are numerically consistent in the sense that they have the same accuracy on the spatial grid as the real-time propagation.

The final important step in the calculation is the analysis of the fully evolved wavefunction. As mentioned above, purely time-dependent techniques must confront the difficulty of projecting the propagated asymptotic wavefunction onto the known outgoing channels in order to perform an energy or momentum analysis. In the present case, these outgoing waves are a superposition of the so-called Volkov states which describe an electron propagating solely in the presence of an electromagnetic field (Rosenberg 1982):

$$\varphi_{\text{asy}}(x, t) = \int a(k, t) \exp(\mathrm{i}kx) \exp\left(\mathrm{i} \int^t kA(s)\, \mathrm{d}s\right) \exp(\mathrm{i}k^2 t/2m)\, \mathrm{d}k. \tag{6}$$

This analysis is performed by choosing a region of the grid which has only outgoing waves and then determining the k-labelled coefficients $a(k, t)$ by a spatial Fourier transformation of the propagated wavefunction on this isolated section of the grid. Each of these coefficients is stored at each time step.

A technical difficulty remains since the dipole approximation does not allow any spatial dependence of the laser field, yet any experiment performed will have the detector outside the laser field. The analysis outlined above assumes, in essence, that the detector is inside the field region, i.e. that the photoelectron spectrum depends explicitly upon time. There are at least two ways to address this problem: one is to average the projected wavefunction over the entire time interval of the propagation; another is to introduce some spatial variation into the vector potential and then analyse the asymptotic wavefunction in the potential-field-free region. The first method is used in the results presented below. The second of these two methods might not be a consistent procedure since other equally important terms from quantum electrodynamics have been neglected (Knight 1986). Nonetheless, the results of a few runs with a spatially dependent field coincided with the time averaging method.

The time averaging of the coefficients $a(k, t)$ corresponds physically to a detector collecting the ejected-photoelectron wavepacket for a specified length of time and then averaging the results. This method has already been used in other circumstances to compensate for the neglect of the spatial extent of the vector potential (Kroll and Watson 1973).

An attenuating function must be used on the edges of the grid to ensure that the total wavefunction does indeed vanish at the boundary (as required in equation (2)) (Kosloff and Cerjan 1984). The propagated wavefunction eventually fills the chosen grid over the time intervals of interest so that it is necessary to remove the extraneous asymptotic part of the wavefunction. The position and functional form of the attenuating function does not appear to be critical so long as it is sufficiently removed from

the regions of physical interest and no reflections are permitted (the attenuation is not large enough). As the calculation proceeds, the normalisation of the propagated wavefunction decreases with time as the wavefunction reaches the boundary. By monitoring this change as a function of time, the ionisation rate can be calculated.

Since the zero-field stationary states are readily calculated, it is straightforward to evaluate the projections of the evolving wavefunction on these states. These quantities indicate the relative importance of different mechanisms for ionisation—either directly from the ground state or by intermediate excitation to the higher lying bound state. In the presence of the laser field, these states are greatly modified, but projections onto them do yield some insight into the deviation of the system from adiabatic conditions.

In summary, the methodology is to first calculate the zero-field stationary states in the static well; the initial state is chosen to be the ground state of the system, which is then propagated by using the psuedospectral algorithm with explicit time differencing in the presence of the time varying fields; finally, the wavefunction is collected at the edge of the spatial grid and analysed to obtain the ionisation rate and various projections.

4. Results

The techniques described above were used to investigate the frequency and intensity dependence of the ionisation rates and ejected-photoelectron spectra. Table 1 gives the values of the numerical constants chosen for the spatial grid and time step. The asymptotic analysis was performed using N_{an} points in a region starting at $\pm 50\ a_0$. As will be seen, this choice of analysis points does not provide high-energy resolution in the spectra but it is sufficient to demonstrate the overall features of the interaction. The numerical constants were selected to provide a balance between accuracy and computational speed. Further refinement of the grid and time step was tested at high intensity and does not qualitatively change the results.

Table 1. Numerical grid constants.

Grid constant	Value
N_{pts}	1024
N_{an}	256
Δx	$0.4\ a_0$
Δt	0.02 atomic time units

Three different intensities and two photon frequencies were used which correspond to two-photon ($\omega_p = 0.236$ Hartree) and four-photon ($\omega_p = 0.118$ Hartree) ionisation. Figures 1(a)-(f) and 2(a)-(f) display results for $\omega_p = 0.118$ and 0.236 Hartree, respectively, at a laser field intensity of 1×10^{14} W cm^{-2}. Time-dependent phenomena are shown in figures 1(a)-(d) and 2(a)-(d). Figures 1(a) and 2(a) depict the energy absorbed by the particle. The absolute magnitudes of the projections upon the ground and first excited stationary states of the zero-field bound particle are plotted in figures 1(b)-(c) and 2(b)-(c), and the rate of decay, or normalisation change of the

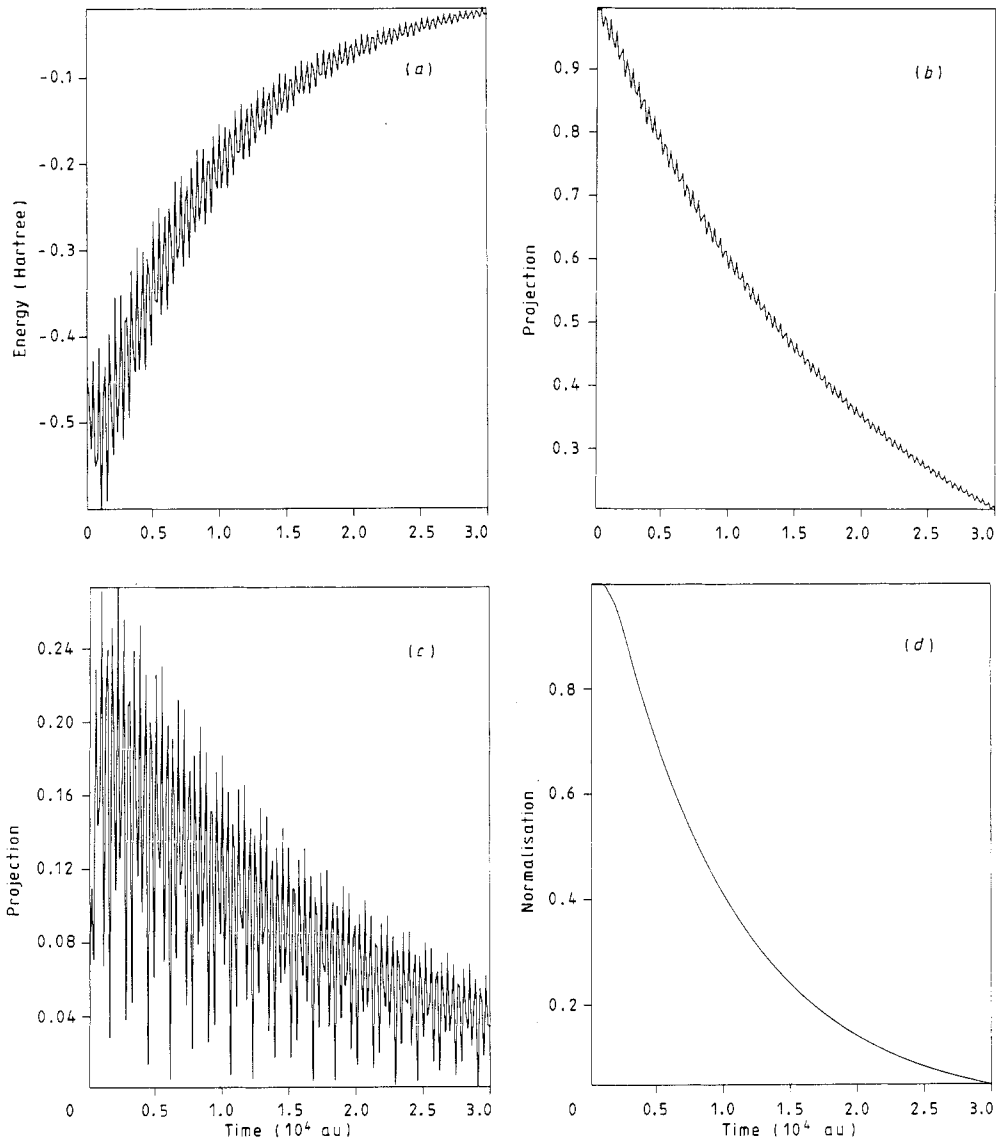

Figure 1. (*a*) Energy absorption as a function of time for $\omega_p = 0.118$ Hartree with a laser intensity of 1×10^{14} W cm^{-2}. (*b*) Absolute value of the projection of the evolving wavefunction upon the ground state as a function of time for $\omega_p = 0.118$ Hartree and 10^{14} W cm^{-2}. (*c*) As (*b*) for the first excited state. (*d*) Normalisation change or ionisation probability as a function of momentum for $\omega_p = 0.118$ Hartree and 10^{14} W cm^{-2}. (*e*) Ejected-photoelectron spectrum as a function of momentum for $\omega_p = 0.118$ Hartree and 10^{14} W cm^{-2}. (*f*) As (*e*) as a function of energy.

wavepacket, are given in figures 1(*d*) and 2(*d*). The plots in figures 1(*e*)-(*f*) and 2(*e*)-(*f*) are derived from the asymptotic Fourier analysis of the evolving wavepacket as a function of momentum and energy. A comparison of the various time plots reveals a difference in mechanism between the two frequencies: the four-photon transition occurs much more adiabatically than the sudden jump for the two-photon transition. Furthermore, the first excited state is essentially unpopulated throughout the higher

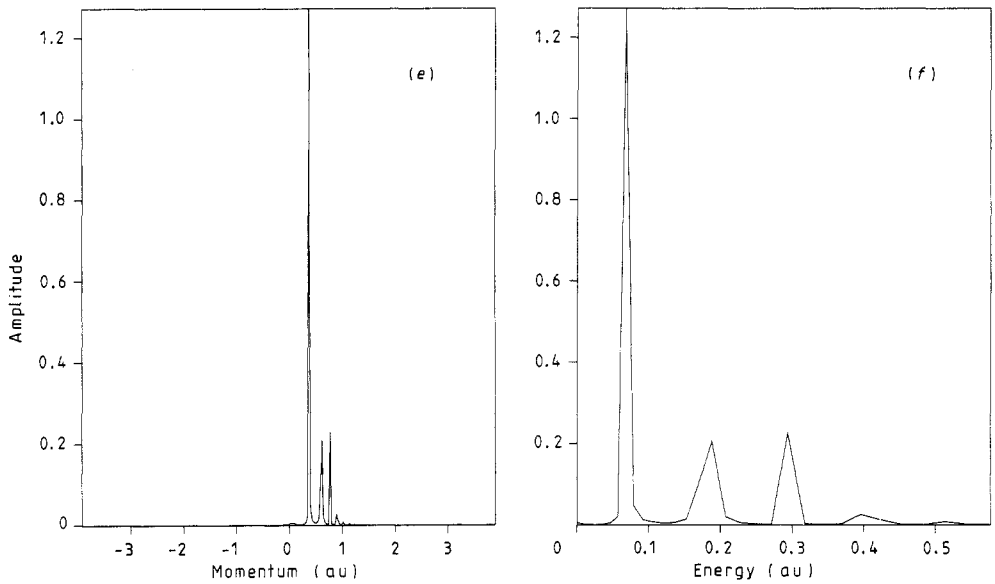

Figure 1. (continued)

frequency ionisation process while it contributes much more to the lower frequency process. These same effects persist for the other intensities examined. The normalisation changes fit an exponential form reasonably well and a one-parameter fit to the time decay was chosen as the predicted decay rate.

Table 2 summarises the ionisation rates as a function of the frequency and intensity of the applied field. Saturation of the ionisation transition has occurred for all intensities and the dependence is not a simple scaling or power law dependence. In fact, the rates for the two-photon ionisation process are almost insensitive to variation in the intensity greater than a factor of ten.

Figures 1(e)-(f) and 2(e)-(f) depict the calculated ejected-photoelectron spectra as a function of either momentum or energy. The absence of negative-momentum peaks in the positive outgoing direction indicates that no numerical contamination of the asymptotic analysis occurred. As mentioned above, the energy resolution is insufficient to locate the positions of the peaks with a high degree of accuracy. It is sufficient, nonetheless, to display the separate photon absorption peaks and their relative intensities. There is a clear difference again in the two cases: a large multiplicity of peaks is seen for the lower frequency.

A summary of the ejected-photoelectron peaks as a function of energy and intensity is given in table 3. The number of peaks observed increases as the intensity increases for a fixed frequency and as the photon frequency decreases for a fixed intensity. These results indicate that multiphoton processes beyond those needed for ionisation become more probable at higher intensities. Within the numerical uncertainty of the calculation, the peaks are separated by single-photon processes. Also, no peak suppression is observed in any of the cases (Kruit *et al* 1983).

In order to demonstrate the generality of the technique, a spatial dependence was introduced into the vector potential of the form

$$A(x, t) = 2A(t)\cos(\omega_p t)/[1+\exp(\alpha x^2)]. \tag{7}$$

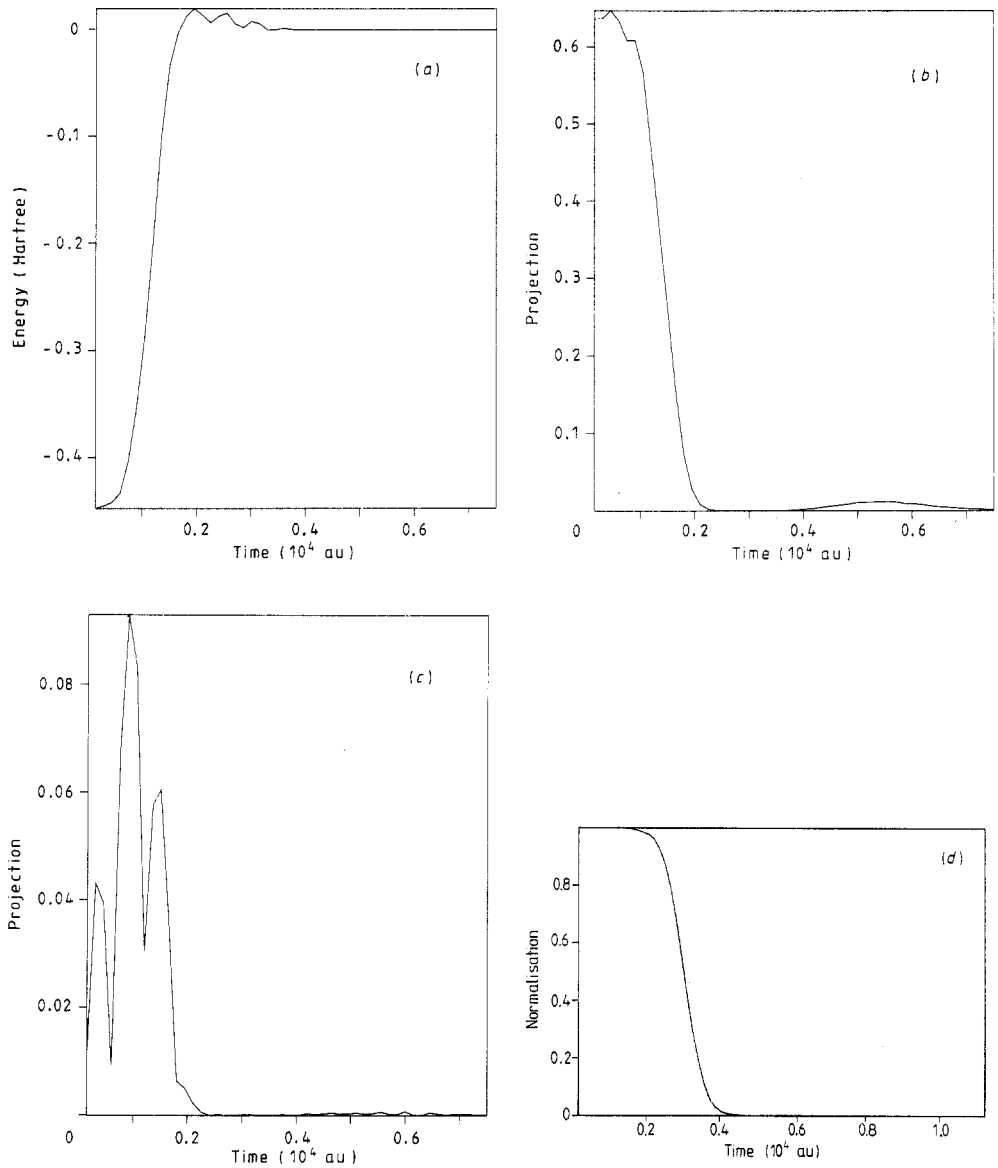

Figure 2. (continued)

The only substantive change in the previous calculations was the inclusion of a single derivative term ($n = 1$ in equation (2)). Since this inclusion necessitates two more FFT operations per cycle, the running time increases by about a factor of two. Table 4 contains the results of the spatial dependence at 10^{14} W cm^{-2} for the two photon frequencies and $\alpha = 0.002$. Neither the ionisation rates nor photoelectron spectra change dramatically.

As a final test of the results, the number of field cycles used to turn the laser field on was increased tenfold so that a in equation (5) was equal to 200π. One calculation was performed for the case where $\omega_p = 0.236$ Hartree and the intensity was equal to 1×10^{14} W cm^{-2}. The ionisation rate and the photoelectron spectrum did not change.

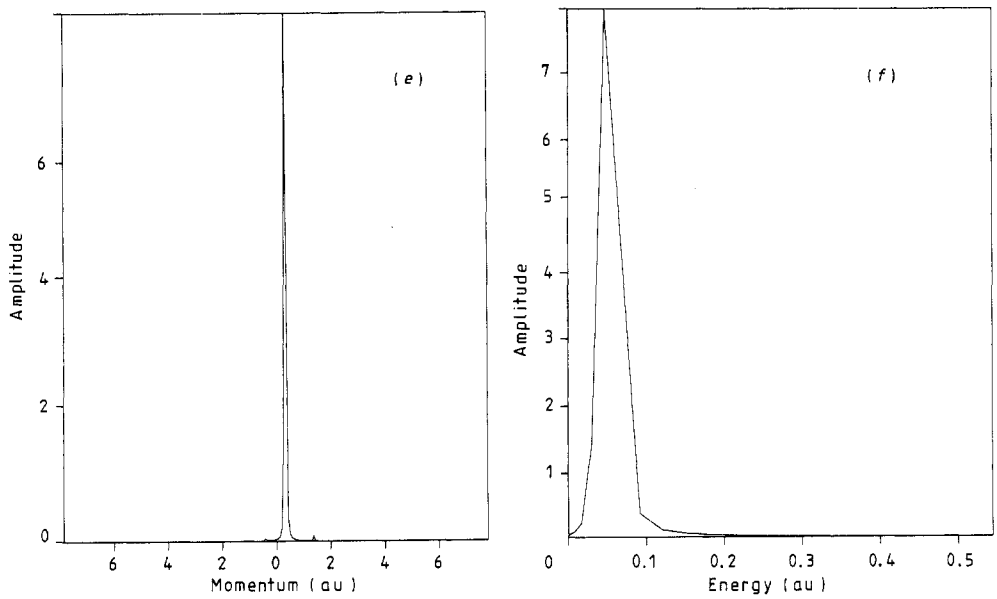

Figure 2. (*a*)-(*f*) Same as corresponding figure 1 quantities for $\omega_p = 0.236$ Hartree.

Table 2. Ionisation rates (s^{-1}) as a function of photon frequency and laser field intensity.

	ω_p (Hartree)	
	0.118	0.236
Intensity (10^{13} W cm^{-2})	Ionisation rate (10^{13} s^{-1})	
1	9.6×10^{-4}	3.9
5	6.3×10^{-2}	5.1
10	4.4×10^{-1}	6.2

5. Discussion

The intensity and frequency dependence of the ejected-photoelectron spectra are not adequately described by simple first-order perturbation theory. Most treatments of photoionisation produce an expression for the transition probability w which has the general form (Reiss 1980, Keldysh 1964)

$$W = \sum_n f(n, \omega, k)|J_n(k\beta)|^2 \delta(k^2/2m + E_b - n\omega) \tag{8}$$

where E_b is the energy of the bound state, $\beta = (A_0/\omega c)$, and the function $f(n, \omega, k)$ is a slowly varying function of its arguments. Thus, the major features of the ionisation process are controlled by the delta function and Bessel function factors. Using the fixed-order, small-argument approximation for the integral-order Bessel function

$$J_n(z) \simeq (z/2)^n/n! \tag{9}$$

and the relevant values for the cases considered above, equation (8) produces negligible transition probabilities which disagree by several orders of magnitude with the calculated results.

Table 3. Ratio of the ejected-photoelectron peak intensity as a function of energy (all peaks scaled to the largest value).

	ω_p (Hartree)			
	0.118		0.236	
Intensity (10^{13} W cm^{-2})	Energy (Hartree)	Ratio	Energy (Hartree)	Ratio
1	0.012	1.0	0.017	1.0
	0.120	1.3×10^{-2}	0.228	2.9×10^{-3}
5	0.092	1.0	0.008	1.0
	0.208	0.88	0.188	2.5×10^{-2}
	0.318	8.8×10^{-2}		
10	0.068	1.0	0.002	1.0
	0.188	0.17	0.188	0.23
	0.294	0.18	0.424	7.1×10^{-3}
	0.396	2.2×10^{-2}		
	0.513	7.6×10^{-3}		
	0.640	3.1×10^{-3}		
	0.750	1.6×10^{-3}		

Table 4. Effect of the inclusion of spatial variation in the vector potential at 1×10^{14} W cm^{-2}.

ω_p (Hartree)			
0.118		0.236	
Ionisation rate (10^{13} s^{-1})			
0.39		2.3	
E (Hartree)	Ratio of peaks	E (Hartree)	Ratio of peaks
0.068	1.0	0.008	1.0
0.153	0.41	0.188	0.22
0.272	0.32	0.424	6.9×10^{-3}
0.369	0.25		
0.482	1.6×10^{-2}		
0.610	7.1×10^{-3}		

A comparison of the linearly forced harmonic oscillator is also useful as a corroborative test of the adiabaticity of the system. That is, by calculating the time-dependent transition probability from the ground to first excited state and comparing it with the projections in figures 1 and 2, it is clear that the bound particle is held briefly by the harmonic restoring force for the high-frequency case with little population of the zero-field first excited state. The opposite situation holds for the low-frequency case, which shows a behaviour similar to the full harmonic oscillator results. The exact probability is shown in figure 3 (calculated following Pechukas and Light 1966) for $\omega_p = 0.118$ Hartree and 10^{14} W cm^{-2}. The temporal initialisation was chosen to be linear for 10 cycles of the field for computational convenience. These comparisons

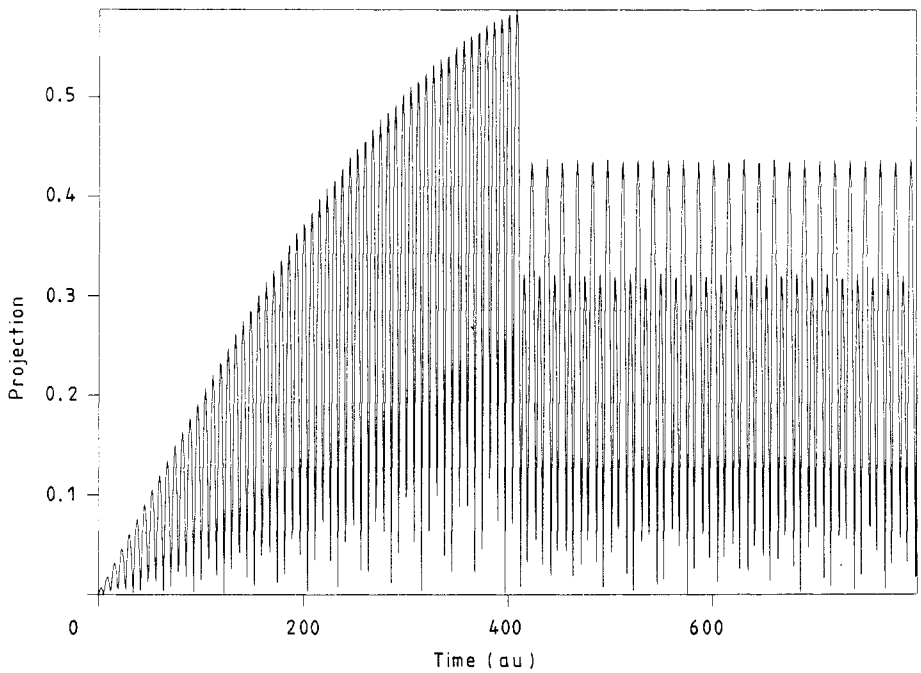

Figure 3. Transition probability between ground and first excited states of a linearly forced harmonic oscillator as a function of time for $\omega_p = 0.118$ Hartree and 10^{14} W cm^{-2}.

indicate that the approach of the system to full ionisation is qualitatively different for different frequencies even at large field intensities.

The purpose of this work is to demonstrate a general computational approach to the investigation of photon-particle interactions within the context of a one-dimensional-model problem. This technique provides a natural way to incorporate several experimentally relevant features of these interactions and to reach a natural interpretation of the results obtained. The major limitations of the method are the number of spatial-grid points necessary and the size of the time step. As the cases outlined earlier show, the spreading of the wavefunction and the asymptotic analysis require a large number of grid points for the resolution of the photoelectron spectra. The memory and time requirements become prohibitive if too fine a resolution is demanded. The time step is essentially determined from numerical stability considerations, which can become quite severe if the grid spacing is small or the wavepacket evolves very slowly. For example, for low-frequency photons and low-intensity fields, the wavepacket propagates so slowly that very large amounts of computer time are necessary to complete the calculation. In the results presented here, both of these limitations were present.

Finally, it should also be emphasised that the one-dimensional model considered here has limited applicability to experimental observation. First, the restriction to one dimension is an impossible situation for an electromagnetic wave interacting with matter since the field and its direction of propagation cannot lie along the same axis. Obviously angular distributions and geometric (solid-angle) effects cannot be included.

The extension of the one-dimensional results to higher dimensions is straightforward for potentials of limited spatial extent without singularities—for example, a cut-off

harmonic oscillator in three dimensions. The important case of the Coulomb potential requires an exponential mesh and the use of Hankel transforms, which is an extension of the technique presented here.

Another, more serious, limitation of the present model is that it is strictly a one-particle model, i.e. electron correlation or many-body effects are not included. It is also important to assess the effect of changing the potential to a Coulombic force, even for the electron model studies. However, the overall qualitative effects of the intensity and frequency dependence of the particle motion should serve as a guide to the behaviour of particles in more realistic situations. Techniques such as the one above or similar (Kulander 1987) show promise for extension into the domain of complex, three-dimensional interactions.

Acknowledgments

Drs K Kulander and B W Shore provided considerable insight into the nature of particle–field interactions over the course of many conversations. Dr A Szoke supplied the stimulus for these investigations and suggested the model potential form chosen. It is a pleasure to thank them for their contributions. This work was performed under the auspices of the US Department of Energy by the Lawrence Livermore National Laboratory under contract No. W-7405-ENG-48. Research at the Fritz Haber Institute is partially supported by the Minerva Gesellschaft für die Forschung, Munich, West Germany.

References

Chu S-I 1978 *Chem. Phys. Lett.* **54** 367
—— 1985 *Adv. Mol. Phys.* **21** 197
Feit M D, Fleck J A and Steiger A 1982 *J. Comp. Phys.* **47** 412
Geltman S 1977 *J. Phys. B: At. Mol. Phys.* **10** 831
Keldysh L V 1964 *Zh. Eksp. Teor. Fiz.* **47** 1945 and 1965 *Sov. Phys.—JETP* **20** 1307
Knight P 1986 Private communication
Kosloff R and Cerjan C 1984 *J. Chem. Phys.* **81** 3722
Kosloff D and Kosloff R 1983 *J. Comp. Phys.* **52** 35
Kroll N M and Watson K M 1973 *Phys. Rev.* A **8** 804
Kruit P, Kinman J, Muller H G and van der Wiel M J 1983 *Phys. Rev.* A **28** 248
Kulander K 1987 *Phys. Rev.* A **35** 445
Lambropolous P 1985 *Phys. Rev. Lett.* **55** 2141
Lambropolous P and Smith S J (eds) 1985 *Multiphoton Processes* (New York: Springer)
L'Huillier A, Jonsson L and Wendin G 1986 *Phys. Rev.* A **33** 3938
Lompre L A, L'Huillier A, Mainfray G and Manus C 1985 *J. Opt. Soc. Am.* B **2** 1906
Luk T S, Johann U, Egger H, Pummer H and Rhodes C K 1985 *Phys. Rev.* A **32** 214
Muller H G and Tip A 1984 *Phys. Rev.* A **30** 3039
Pechukas P and Light J C 1966 *J. Chem. Phys.* **44** 3897
Reiss H R 1980 *Phys. Rev.* A **22** 1786
Rosenberg L 1982 *Adv. At. Mol. Phys.* **18** 1
Shakeshaft R 1983 *Phys. Rev.* A **28** 667
Tal-Ezer H and Kosloff R 1984 *J. Chem. Phys.* **81** 3967